Available online at www.sciencedirect.com

SCIENCE DIRECT®

Communications in Nonlinear Science and Numerical Simulation 11 (2006) 326–339

Communications in Nonlinear Science and Numerical Simulation

www.elsevier.com/locate/cnsns

An analytic solution of unsteady boundary-layer flows caused by an impulsively stretching plate

Shijun Liao

School of Naval Architecture, Ocean and Civil Engineering, Shanghai Jiao Tong University, Shanghai 200030, China

Received 31 August 2004; received in revised form 31 August 2004; accepted 3 September 2004
Available online 21 November 2004

Abstract

In this paper, the unsteady boundary-layer flows caused by an impulsively stretching flat plate is solved by means of an analytic approach. Unlike perturbation techniques, this approach gives accurate analytic approximations uniformly valid for all dimensionless time. Besides, a simple but accurate analytic formula for the local skin friction is given, which agrees well with numerical results and thus is useful in the related industries. To the best of our knowledge, this type of analytic solutions has been never reported. Furthermore, the proposed analytic approach has general meaning and therefore may be applied in the similar way to other unsteady boundary-layer flows to get accurate analytic solutions valid for all time.

PACS: 47.15.Cb; 46.15.Ff
Keywords: Unsteady; Boundary-layer flows; Stretching plate; Impulsive motion

1. Introduction

The investigation of the boundary-layer flows of an incompressible fluid over a stretching surface has many important applications in engineering, such as the aerodynamic extrusion of plastic sheets, the boundary layer along a liquid film condensation process, the cooling process of metallic plate in a cooling bath, and in the glass and polymer industries. The investigation were made by

E-mail address: sjliao@sjtu.edu.cn

1007-5704/$ - see front matter
doi:10.1016/j.cnsns.2004.09.004

many researchers, including Sakiadis [1], Crane [2], Banks [3], Banks and Zaturska [4], Grubka and Bobba [5], Ali [6] for the impermeable plate, and Erickson et al. [7], Gupta and Gupta [8], Chen and Char [9], Chaudhary et al. [10], Elbashbeshy [11], Magyari and Keller [12] for the permeable plate. The unsteady boundary layers due to an impulsively started flat plate were considered by some researchers [13–18]. However, the work on the unsteady boundary-layer flows due to an impulsively stretching surface in a viscous fluid [19,20,18,21] is relatively little. Currently, Nazar et al. [21] solved the unsteady boundary-layer flow due to an impulsively stretching surface in a rotating fluid by means of a transformation found by Williams and Rhyne [22] and the so-called Keller-box numerical method, and they obtained a first-order perturbation approximation.

It seems hard to obtain analytic solutions of unsteady boundary-layer flows, which are valid for *all* time. Perturbation techniques are applied by many researchers, but the corresponding analytic solutions are valid only for small time [16,18,21]. To the best of our knowledge, no one has reported any analytic solutions of unsteady boundary-layer flows over a semi-infinite flat plate, which are valid and accurate for *all* time.

Currently, an analytical method for strongly nonlinear problems, namely the Homotopy Analysis Method [23], has been developed and successfully applied to many kinds of nonlinear problems in science and engineering [24–33]. In this paper, the Homotopy Analysis Method is employed to give an analytic solution of the unsteady boundary-layer flows caused by a impulsively stretching plate, which is valid and accurate for all time.

2. Mathematical description

Consider an unsteady boundary layer developed by an impulsively stretching plate in a constant pressure viscous flow, governed by

$$\frac{\partial u}{\partial t}+u\frac{\partial u}{\partial x}+v\frac{\partial u}{\partial y}=\nu\frac{\partial^2 u}{\partial y^2}, \tag{1}$$

$$\frac{\partial u}{\partial x}+\frac{\partial v}{\partial y}=0, \tag{2}$$

subject to the boundary conditions

$$t\geqslant 0:\quad u=ax,\quad v=0\quad \text{at}\quad y=0, \tag{3}$$

$$u\to 0\quad \text{as } y\to+\infty \tag{4}$$

where $a > 0$, and the initial conditions

$$t=0:\quad u=v=0\quad \text{at all points } (x,y). \tag{5}$$

Let ψ denote the stream function. Following Seshadri et al. [18] and Nazar et al. [21], we use Williams and Rhyne's similarity transformation [22]

$$\psi=\sqrt{a\nu\xi}\,xf(\eta,\xi),\quad \eta=\sqrt{\frac{a}{\nu\xi}}\,y,\quad \xi=1-\exp(-\tau),\quad \tau=a\,t. \tag{6}$$

The original equations become

$$\frac{\partial^3 f}{\partial \eta^3}+\frac{1}{2}(1-\xi)\eta\frac{\partial^2 f}{\partial \eta^2}+\xi\left[f\frac{\partial^2 f}{\partial \eta^2}-\left(\frac{\partial f}{\partial \eta}\right)^2\right]=\xi(1-\xi)\frac{\partial^2 f}{\partial \eta \partial \xi},\quad \xi \geqslant 0, \tag{7}$$

subject to the boundary conditions

$$f(0,\xi)=0,\quad \left.\frac{\partial f}{\partial \eta}\right|_{\eta=0}=1,\quad \left.\frac{\partial f}{\partial \eta}\right|_{\eta=+\infty}=0. \tag{8}$$

When $\xi = 0$, corresponding to $\tau = 0$, (7) becomes the Rayleigh type of equation

$$\frac{\partial^3 f}{\partial \eta^3}+\frac{1}{2}\eta\frac{\partial^2 f}{\partial \eta^2}=0, \tag{9}$$

subject to

$$f(0,0)=0,\quad \left.\frac{\partial f}{\partial \eta}\right|_{\eta=0,\xi=0}=1,\quad \left.\frac{\partial f}{\partial \eta}\right|_{\eta=+\infty,\xi=0}=0. \tag{10}$$

The above equation has the exact solution

$$f(\eta,0)=\eta\,\mathrm{erfc}(\eta/2)+\frac{2}{\sqrt{\pi}}\left[1-\exp(-\eta^2/4)\right], \tag{11}$$

where $\mathrm{erfc}(\eta)$ is the error function defined by

$$\mathrm{erfc}(\eta)=\frac{2}{\sqrt{\pi}}\int_{\eta}^{+\infty}\exp(-z^2)\,\mathrm{d}z.$$

When $\xi = 1$, corresponding to $\tau \to +\infty$, we have from Eq. (7) that

$$\frac{\partial^3 f}{\partial \eta^3}+f\frac{\partial^2 f}{\partial \eta^2}-\left(\frac{\partial f}{\partial \eta}\right)^2=0, \tag{12}$$

subject to

$$f(0,1)=0,\quad \left.\frac{\partial f}{\partial \eta}\right|_{\eta=0,\xi=1}=1,\quad \left.\frac{\partial f}{\partial \eta}\right|_{\eta=+\infty,\xi=1}=0. \tag{13}$$

The above equation has the exact solution

$$f(\eta,1)=1-\exp(-\eta). \tag{14}$$

So, as ξ increases from 0 to 1, $f(\eta,\xi)$ varies from the initial solution (11) to the steady solution (14). Note that, although $f'(+\infty,\xi)\to 0$ exponentially for all ξ, where the prime denotes the differentiation with respect to η, $f'(+\infty,0)$ of the initial solution (11) tends to 0 much more quickly than $f'(+\infty,1)$ of the steady solution (14). So, mathematically, the initial solution (11) is different in essence from the steady one (14). This might be the reason why it is so hard to give an accurate analytic solution uniformly valid for all time $0 \leqslant \tau < +\infty$.

When $\xi = 0$ and $\xi = 1$, we have

$$\left.\frac{\partial^2 f}{\partial \eta^2}\right|_{\eta=0,\xi=0} = -\frac{1}{\sqrt{\pi}} \tag{15}$$

and

$$\left.\frac{\partial^2 f}{\partial \eta^2}\right|_{\eta=0,\xi=1} = -1, \tag{16}$$

respectively. The skin friction coefficient is given by

$$c_f^x(x,\xi) = (\xi Re_x)^{-1/2} f''(0,\xi), \quad 0 \leqslant \xi \leqslant 1, \tag{17}$$

where $Re_x = ax^2/v$ is the local Reynolds number.

3. Perturbation solution

Regard ξ as small parameter. Like Seshadri et al. [18] and Nazar et al. [21], we have the perturbation expression

$$f(\eta,\xi) = g_0(\eta) + g_1(\eta)\xi + g_2(\eta)\xi^2 + \cdots .$$

Substituting it into Eqs. (7) and (8), we obtain the zero-order equation

$$g_0'''(\eta) + \frac{\eta}{2} g_0''(\eta) = 0, \quad g_0(0) = 0, \quad g_0'(0) = 1, \quad g_0'(+\infty) = 0, \tag{18}$$

and the kth-order ($k \geqslant 1$) equation

$$g_k'''(\eta) + \frac{\eta}{2} g_k''(\eta) - k g_k'(\eta) = \frac{\eta}{2} g_{k-1}''(\eta) - (k-1) g_{k-1}'(\eta) - \sum_{i=0}^{k-1} \left[g_i(\eta) g_{k-1-i}''(\eta) - g_i'(\eta) g_{k-1-i}'(\eta) \right], \tag{19}$$

subject to the boundary conditions

$$g_k(0) = g_k'(0) = g_k'(+\infty) = 0. \tag{20}$$

The solution of the Rayleigh type of equation (18) is

$$g_0(\eta) = f(\eta,0) = \eta\, \mathrm{erfc}(\eta/2) + \frac{2}{\sqrt{\pi}} \left[1 - \exp(-\eta^2/4)\right].$$

Substituting it into Eqs. (19) and (20), we obtain

$$\begin{aligned} g_1(\eta) = {} & \left(\frac{1}{2} - \frac{2}{3\pi}\right) \left[\left(1 + \frac{\eta^2}{2}\right) \mathrm{erfc}(\eta/2) - \frac{\eta}{\sqrt{\pi}} \mathrm{e}^{-\eta^2/4} \right] - \frac{1}{2}\left(1 - \frac{\eta^2}{2}\right) \mathrm{erfc}^2(\eta/2) \\ & - \frac{3\eta}{2\sqrt{\pi}} \mathrm{e}^{-\eta^2/4} \mathrm{erfc}(\eta/2) - \frac{1}{\sqrt{\pi}} \left(\frac{4}{3\sqrt{\pi}} - \frac{\eta}{4}\right) \mathrm{e}^{-\eta^2/4} + \frac{2}{\pi} \mathrm{e}^{-\eta^2/2}. \end{aligned} \tag{21}$$

Obviously, $g_k(\eta)$ can be expressed by the following set of base functions

$$\left\{\eta^m \exp\left(-\frac{n\eta^2}{4}\right)\mathrm{erfc}^j\left(\frac{\eta}{2}\right)\middle| m \geqslant 0,\ \ n \geqslant 0,\ \ j \geqslant 0\right\}. \tag{22}$$

The base functions contain the error function erfc(η/2) and its powers. Note that these base functions appear on the right-hand side of the high-order perturbation equation (19). So, although (19) is a linear differential equation, it is rather difficult to solve when $k \geqslant 2$. Like Seshadri et al. [18] and Nazar et al. [21], we can obtain only the first-order perturbation approximation. Note that, the steady solution (14) when $\xi = 1$ is simply an exponent function. The error function erfc(η/2), which appears in the initial solution (11) when $\xi = 0$, seems too complicated and also unnecessary for the unsteady solution (14). Because only the first-order approximation can be obtained, it is unclear whether or not the simple steady solution (14) can be expressed by the above set of base functions that contain the error function and its powers.

The corresponding skin friction coefficient at the first-order of perturbation approximation is

$$C_f^x(x,\xi) \approx -\frac{1}{\sqrt{\pi\xi Re_x}}\left[1+\left(\frac{5}{4}-\frac{4}{3\pi}\right)\xi\right]. \tag{23}$$

4. Homotopy analytic solution

In this section we employ the homotopy analysis method to solve Eqs. (7) and (8). According to previous discussions, we should avoid the appearance of the error function and its powers so that high-order approximations can be obtained. From (7), (8), (11), and (14), it is reasonable to assume that $f(\eta,\xi)$ could be expressed by the following set of base functions

$$\left\{\xi^k\eta^m\exp(-n\eta)|k \geqslant 0,\ \ m \geqslant 0,\ \ n \geqslant 0\right\} \tag{24}$$

such that

$$f(\eta,\xi) = a_0^{0,0} + \sum_{k=0}^{+\infty}\sum_{m=0}^{+\infty}\sum_{n=1}^{+\infty} a_k^{m,n}\xi^k\eta^m\exp(-n\eta), \tag{25}$$

where $a_k^{m,n}$ is a coefficient. It provides us with the so-called Rule of Solution Expression (see [23,24]). From (7), (8), and (25), it is straightforward to choose the initial approximation

$$f_0(\eta,\xi) = 1 - \exp(-\eta), \tag{26}$$

which is exactly the same as the steady-state solution $f(\eta, 1)$, and the auxiliary linear operator

$$\mathscr{L}[\phi(\eta,\xi;q)] = \frac{\partial^3\phi}{\partial\eta^3} - \frac{\partial\phi}{\partial\eta}, \tag{27}$$

which has the property

$$\mathscr{L}[C_1 + C_2\exp(-\eta) + C_3\exp(\eta)] = 0. \tag{28}$$

From (7), we define the nonlinear operator

$$\mathscr{N}[\phi(\eta,\xi;q)] = \frac{\partial^3\phi}{\partial\eta^3} + \frac{1}{2}(1-\xi)\eta\frac{\partial^2\phi}{\partial\eta^2} + \xi\left[\phi\frac{\partial^2\phi}{\partial\eta^2} - \left(\frac{\partial\phi}{\partial\eta}\right)^2\right] - \xi(1-\xi)\frac{\partial^2\phi}{\partial\eta\partial\xi}. \tag{29}$$

Let $\hbar$ denote a nonzero auxiliary parameter. We construct the so-called zero-order deformation equation (see [23,24])

$$(1-q)\mathscr{L}[\phi(\eta,\xi;q)-f_0(\eta,\xi)] = q\hbar\mathscr{N}[\phi(\eta,\xi;q)], \tag{30}$$

subject to the boundary conditions

$$\phi(0,\xi;q)=0, \quad \left.\frac{\partial\phi(\eta,\xi;q)}{\partial\eta}\right|_{\eta=0}=1, \quad \left.\frac{\partial\phi(\eta,\xi;q)}{\partial\eta}\right|_{\eta=+\infty}=0, \tag{31}$$

where $q\in[0,1]$ is an embedding parameter. Obviously, when $q = 0$ and $q = 1$, we have

$$\phi(\eta,\xi;0)=f_0(\eta,\xi) \tag{32}$$

and

$$\phi(\eta,\xi;1)=f(\eta,\xi), \tag{33}$$

respectively. Thus, as q increases from 0 to 1, $\phi(\eta,\xi;q)$ varies from the initial approximation $f_0(\eta,\xi)$ to the solution $f(\eta,\xi)$ of the original equations (7) and (8). Assume that the auxiliary parameter $\hbar$ is so properly chosen that the Taylor series of $\phi(\eta,\xi;q)$ expanded with respect to the embedding parameter, i.e.

$$\phi(\eta,\xi;q)=\phi(\eta,\xi;0)+\sum_{n=1}^{+\infty}f_n(\eta,\xi)q^n, \tag{34}$$

where

$$f_n(\eta,\xi)=\frac{1}{n!}\left.\frac{\partial^n\phi(\eta,\xi;q)}{\partial q^n}\right|_{q=0}, \tag{35}$$

converges at $q = 1$. Then, we have from (32) and (33) that

$$f(\eta,\xi)=f_0(\eta,\xi)+\sum_{n=1}^{+\infty}f_n(\eta,\xi). \tag{36}$$

Write

$$\vec{f}_n=\{f_0,f_1,f_2,\ldots,f_n\}.$$

Differentiating the zero-order deformation equations (30) and (31) m times with respect to q, then dividing by $m!$, and finally setting $q = 0$, we have the mth-order deformation equations (see [23,24])

$$\mathscr{L}[f_m(\eta,\xi)-\chi_m f_{m-1}(\eta,\xi)]=\hbar R_m(\vec{f}_{m-1},\eta,\xi), \tag{37}$$

subject to the boundary conditions

$$f_m(0,\xi)=0, \quad \left.\frac{\partial f_m(\eta,\xi)}{\partial\eta}\right|_{\eta=0}=0, \quad \left.\frac{\partial f_m(\eta,\xi)}{\partial\eta}\right|_{\eta=+\infty}=0, \tag{38}$$

where

$$R_m(\vec{f}_{m-1}, \eta, \xi) = \frac{\partial^3 f_{m-1}}{\partial \eta^3} + \frac{1}{2}(1-\xi)\eta \frac{\partial^2 f_{m-1}}{\partial \eta^2} - \xi(1-\xi)\frac{\partial^2 f_{m-1}}{\partial \eta \partial \xi} + \xi \sum_{n=0}^{m-1}\left[f_{m-1-n}\frac{\partial^2 f_n}{\partial \eta^2} - \frac{\partial f_{m-1-n}}{\partial \eta}\frac{\partial f_n}{\partial \eta}\right] \quad (39)$$

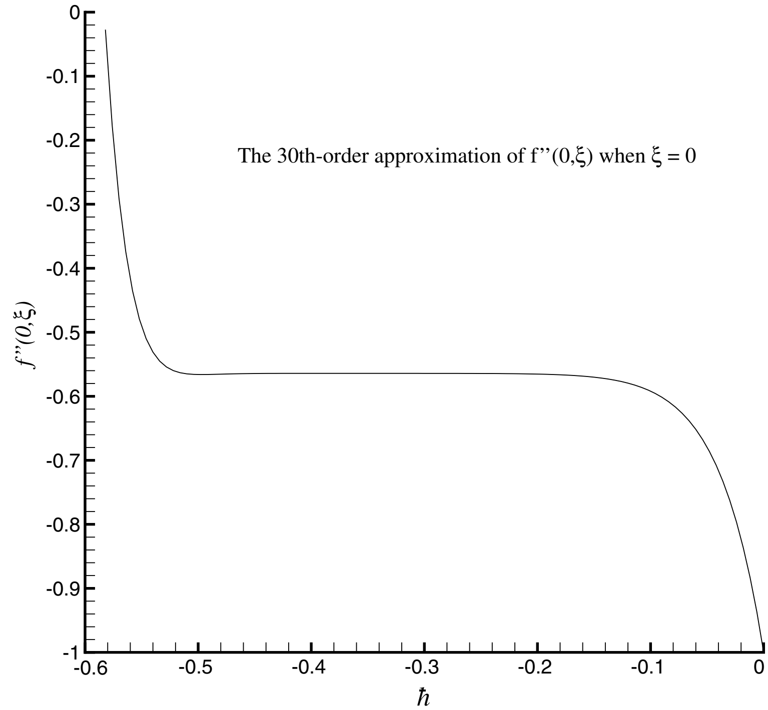

Fig. 1. The $\hbar$-curve of $f''(0)$ when $\xi = 0$.

Table 1
The analytic approximations of $f''(0,0)$ by means of $\hbar = -1/4$

Order of approximation	$f''(0,0)$
5	−0.69303
10	−0.60114
15	−0.57440
20	−0.56693
25	−0.56491
30	−0.56438
35	−0.56424
40	−0.56420
45	−0.56419
50	−0.56419

and

$$\chi_n = \begin{cases} 1, & n > 1, \\ 0, & n = 1. \end{cases} \tag{40}$$

Let $f_m^*(\eta,\xi)$ denote a special solution of Eq. (37). From (28), its general solution reads

$$f_m(\eta,\xi) = f_m^*(\eta,\xi) + C_1 + C_2\exp(-\eta) + C_3\exp(\eta),$$

where the coefficients C_1,C_2, and C_2 are determined by the boundary conditions (38). In this way, it is easy to solve the *linear* equations (37) and (38) successively.

Table 2
The [*m*,*m*] homotopy-Padè approximations of $f''(0,0)$

m	$f''(0,0)$
5	−0.56415
10	−0.56418
15	−0.56419
20	−0.56419
25	−0.56419
30	−0.56419

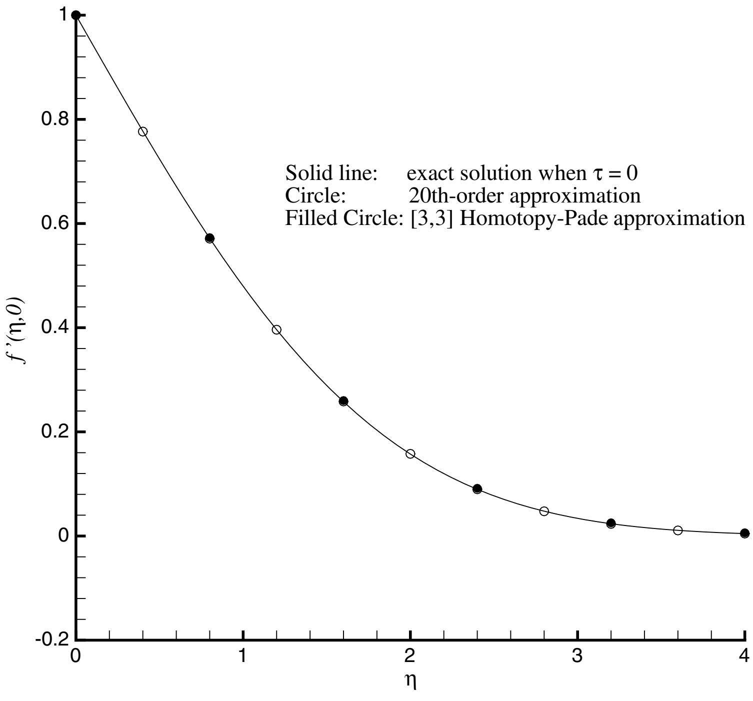

Fig. 2. The comparison of $f'(\eta,0)$ of the exact solution (11) when $\xi = 0$ with the 20th-order approximation when $\hbar = -1/4$ and the [3,3] homotopy-Padé approximation.

Note that, unlike the previous perturbation approach, the special function erfc(η/2) does not appear in the high-order deformation equation (37). So, we can easily obtain results at rather high-order of approximations, especially by means of the symbolic computation software such as Mathematica. In this way, we can obtain accurate analytic approximations uniformly valid for all time τ, as described below.

5. Result analysis

Liao [23] proved that, as long as a solution series given by the homotopy analysis method converges, it must be one of solutions. So, it is important to ensure that the solution series (36) is convergent. Note that the series (36) contains an auxiliary parameter $\hbar$. Obviously, the convergence of the series (36) is determined by this auxiliary parameter. Because the initial approximation (26) is exactly the same as the steady solution (14), it holds when $\xi = 1$ that

$$f_m(\eta, 1) = 0, \quad m = 1, 2, 3, \ldots .$$

Thus, when $\xi = 1$, the solution series (36) is convergent for all $\hbar$. However, when $\xi \neq 1$ such as $\xi = 0$, we had to investigate the influence of $\hbar$ on the convergence of the solution series (36). To do so, we first consider $f''(0, \xi)$, which relates the local skin friction coefficient C_f^x and thus

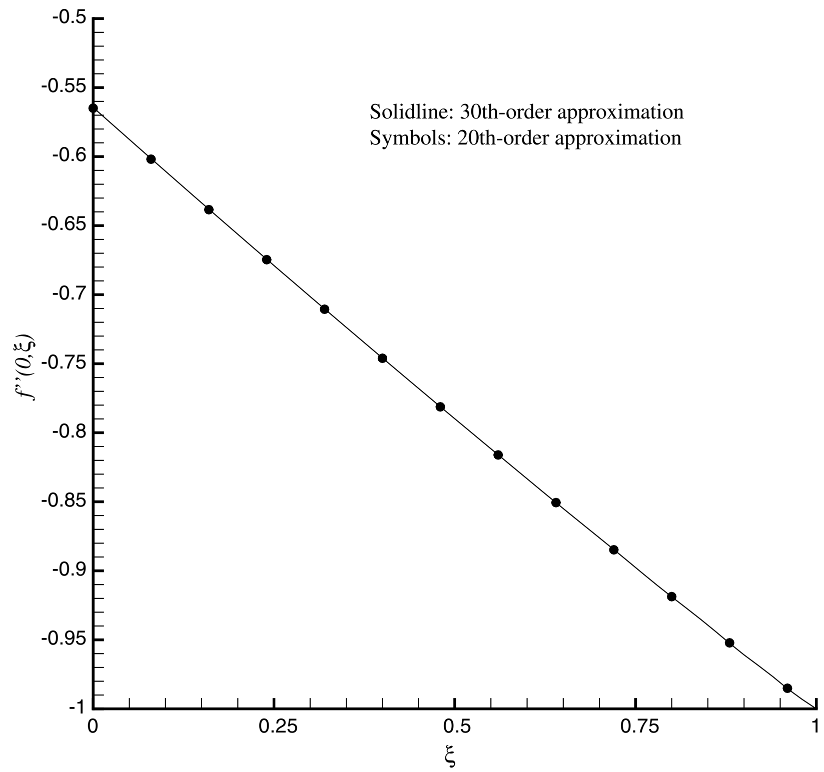

Fig. 3. The approximations of $f''(0, \xi)$ for $0 \leqslant \xi \leqslant 1$ when $\hbar = -1/4$.

has an important physical meaning. Regarding $\hbar$ as an unknown parameter, we can plot curves of $f''(0,\xi)$ via $\hbar$ for different ξ, called the $\hbar$-curves of $f''(0,\xi)$. For example, the $\hbar$-curve of $f''(0,\xi)$ at $\xi = 0$ is as shown in Fig. 1. This $\hbar$-curve has a parallel line segment that corresponds to a region of $-0.35 < \hbar < -0.15$, denoted by $\mathbf{R}_\hbar$. The series of $f''(0,\xi)$ converges, if $\hbar$ is chosen in this region. Indeed, the convergent result of $f''(0,\xi)$ is obtained when $\hbar = -1/4$ and $\xi = 0$, as shown in Table 1. It agrees well with the exact result $f''(0,0) = -1/\sqrt{\pi} \approx -0.56419$. Besides, the convergence can be greatly accelerated by means of the so-called Homotopy-Padé method [23], as shown in Table 2. Furthermore, it is found that, when $\hbar = -1/4$ and $\xi = 0$, the 20th-order approximation and [3,3] homotopy-Padé approximation of the velocity profile $f'(\eta,0)$ agree well with the exact solution (11) in the whole region $0 \leqslant \eta < +\infty$, as shown in Fig. 2. Therefore, the initial solution (11), which contains $\exp(-\eta^2/4)$ and the error function $\mathrm{erfc}(\eta/2)$, can be expressed by the set of the base functions (24).

Similarly, given $\xi \in [0,1]$, we can find a proper value of $\hbar$ to ensure that the solution series (36) is convergent. It is found that, when $\hbar = -1/4$, the solution series (36) is convergent for *any* a value of $\xi \in [0,1]$ in the whole region $0 \leqslant \eta < +\infty$, as shown in Figs. 3 and 4. Note that, the velocity profile varies smoothly as τ increase from 0 to ∞, as shown in Fig. 4. When $\hbar = -1/4$, we have the 30th-order approximation

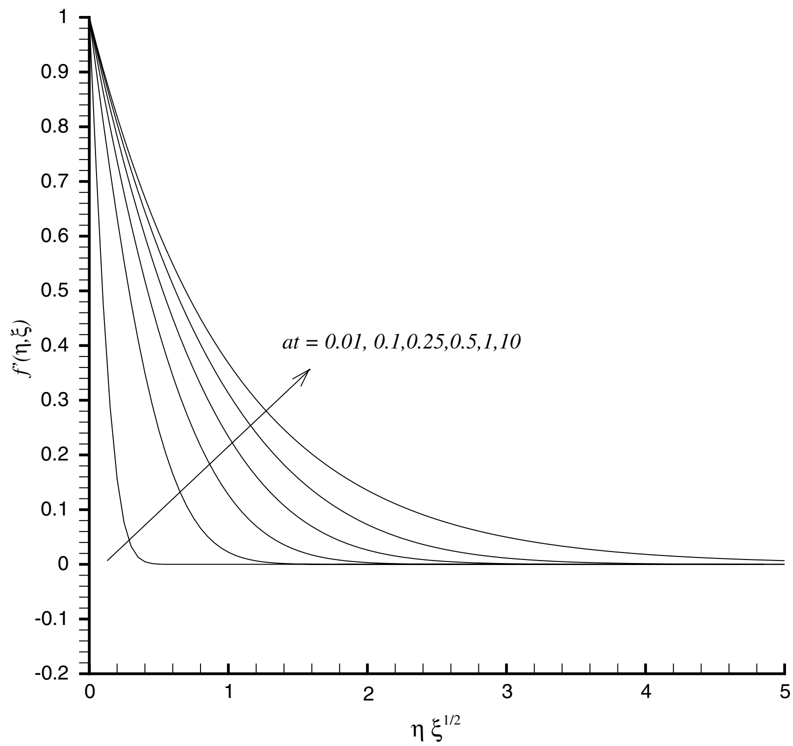

Fig. 4. The velocity profile $f'(\eta,\xi)$ at different dimensionless time $\tau = a\ t$ when $\hbar = -1/4$.

$$
\begin{aligned}
f''(0,\xi) = & -0.5643747892 - 0.4653303619\xi + 2.998049008 \times 10^{-2}\xi^2 - 2.518392990 \times 10^{-3}\xi^3 \\
& - 2.561860658 \times 10^{-5}\xi^4 - 2.531901893 \times 10^{-5}\xi^5 + 3.073353805 \times 10^{-5}\xi^6 \\
& + 5.063224875 \times 10^{-5}\xi^7 + 5.780083670 \times 10^{-5}\xi^8 - 3.019750875 \times 10^{-4}\xi^9 \\
& + 0.2746188078\xi^{10} - 48.017634463\xi^{11} + 3.4358227736 \times 10^3\xi^{12} \\
& - 1.2769915485 \times 10^5\xi^{13} + 2.8257114566 \times 10^6\xi^{14} - 4.0636817506 \times 10^7\xi^{15} \\
& - 6.1471279622 \times 10^{10}\xi^{19} + 1.9058081506 \times 10^{11}\xi^{20} - 4.5980815420 \times 10^{11}\xi^{21} \\
& + 8.6766946108 \times 10^{11}\xi^{22} - 1.2809186178 \times 10^{12}\xi^{23} + 1.4720293398 \times 10^{12}\xi^{24} \\
& - 1.3019682527 \times 10^{12}\xi^{25} + 8.6859786813 \times 10^{11}\xi^{26} - 4.2255442112 \times 10^{11}\xi^{27} \\
& + 1.4139635601 \times 10^{11}\xi^{28} - 2.9087215325 \times 10^{10}\xi^{29} + 2.7723411925 \times 10^9\xi^{30},
\end{aligned}
\tag{41}
$$

which agrees well with the numerical result, as shown in Fig. 3. The corresponding local skin friction at the dimensionless time $\tau \in [0, +\infty)$ agrees with the numerical result, as shown in Fig. 5. Using the first four-terms of expression (41), we have the local skin friction

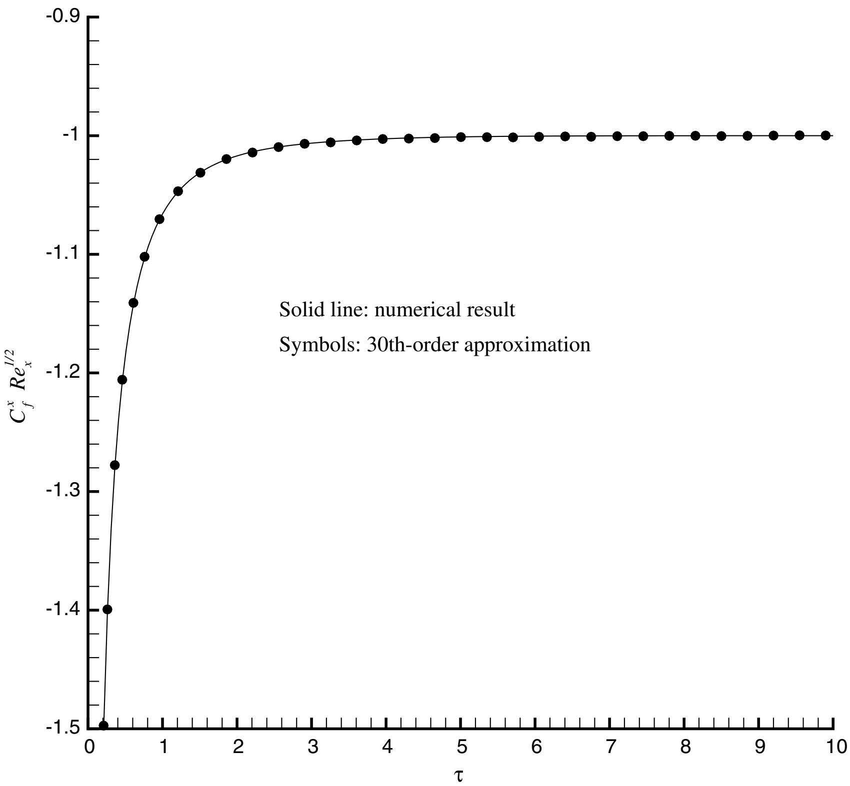

Fig. 5. The comparison of the 30th-order approximation of $C_f^x\sqrt{Re_x}$ at dimensionless time $\tau = a\ t$ with the numerical result.

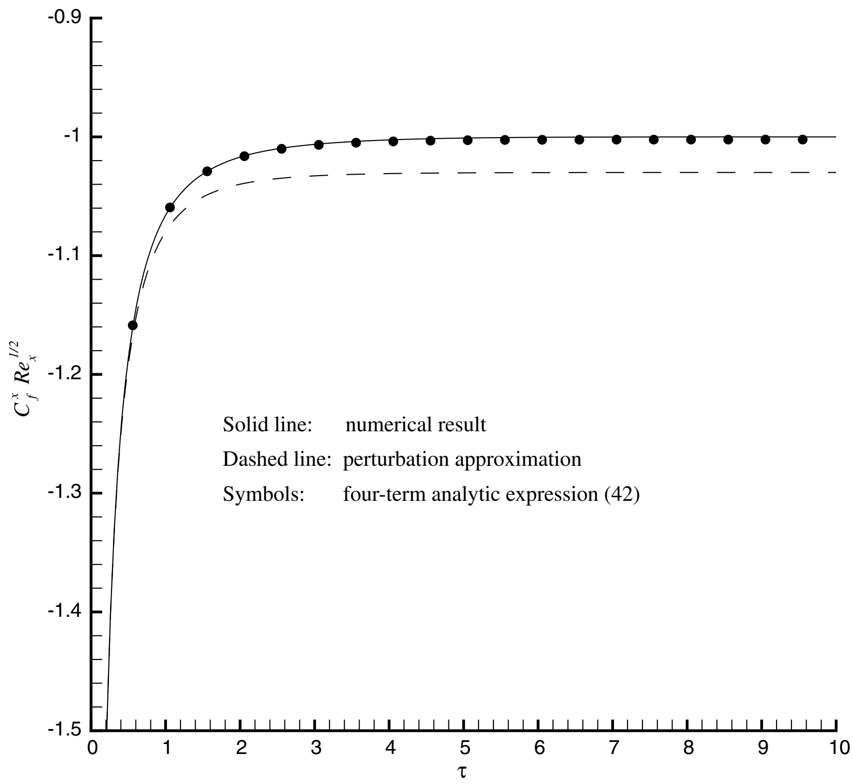

Fig. 6. The comparison of the four-term approximation (42) of $C_f^x\sqrt{Re_x}$ at dimensionless time $\tau = a\,t$ with the numerical result.

$$C_f^x(x,\xi) = (\xi Re_x)^{-1/2}(-0.5643747892 - 0.4653303619\xi + 2.998049008\times 10^{-2}\xi^2 - 2.518392990\times 10^{-3}\xi^3). \tag{42}$$

Even this simplified analytic expression agrees well with the numerical result for all time $0 \leqslant \tau < +\infty$, as shown in Fig. 6. Thus, by means of choosing $\hbar = -1/4$, we obtain an accurate analytic solution uniformly valid for all time $0 \leqslant \tau < +\infty$ in the whole region $0 \leqslant \eta < +\infty$. To the best of our knowledge, such a kind of analytic solution has never been reported.

It should be emphasized that the solution series diverges when $\hbar = -1$ but converges when $\hbar = -1/4$. So, it is the auxiliary parameter $\hbar$ that provides us with a simple way to insure the convergence of the solution series. This is an advantage of the homotopy analysis method.

6. Conclusion

In this paper, the unsteady boundary-layer flows caused by an impulsively stretching flat plate is solved by means of an analytic technique, namely the homotopy analysis method [23]. Unlike perturbation techniques, our approach gives accurate analytic solutions uniformly valid for *all* dimensionless time $0 \leqslant \tau < +\infty$ in the whole region $0 \leqslant \eta < +\infty$. Besides, an analytic formula (41) at the 30th-order of approximation for the local skin friction is given, which agrees well with numerical results. And even the four-term expression (42) of the local skin friction is accurate and valid for all time $0 \leqslant \tau < +\infty$, and thus is useful in the related industries mentioned at the beginning of this paper. To the best of our knowledge, such kind of analytic solutions has never been reported.

There exist many similar unsteady boundary-layer flows and related heat transfer problems, such as the unsteady Blasius boundary-layer flows, unsteady Falkner–Skan boundary-layer flows, unsteady von Kármán swirling viscous flows, and so on. Most of these unsteady boundary-layer flows can be solved in the similar way without difficulties. So, this article provides us with a general approach to get accurate analytic solutions of unsteady boundary-layer flows, which are uniformly valid for all time.

Acknowledgement

Thanks to "National Science Fund for Distinguished Young Scholars" (Approval No. 50125923) of Natural Science Foundation of China, and Li Ka Shing Foundation (Cheung Kong Scholars Programme) for the financial support. Thanks to Prof. Ioan Pop for providing the author with some valuable references.

References

[1] Sakiadis BC. Boundary layer behavior on continuous solid surface. AIChE J 1961;7:26–8.
[2] Crane L. Flow past a stretching plate. Z Angew Math Phys 1970;21:645–7.
[3] Banks WHH. Similarity solutions of the boundary-layer equations for a stretching wall. J Mec Theor Appl 1983;2:375–92.
[4] Banks WHH, Zaturska MB. Eigensolutions in boundary-layer flow adjectent to a stretching wall. IMA J Appl Math 1986;36:263–73.
[5] Grubka LJ, Bobba KM. Heat transfer characteristics of a continuous stretching surface with variable temperature. ASME J Heat Transfer 1985;107:248–50.
[6] Ali ME. Heat transfer characteristics of a continuous stretching surface. Wärme Stoffübertrag 1994;29:227–34.
[7] Erickson LE, Fan LT, Fox VG. Heat and mass transfer on a moving continuous flat plate with suction or injection. Indust Eng Chem 1996;5:19–25.
[8] Gupta PS, Gupta AS. Heat and mass transfer on a stretching sheet with suction or blowing. Canada J Chem Eng 1977;55:744–6.
[9] Chen CK, Char MI. Heat and mass transfer on a continuous stretching surface with suction or blowing. J Math Anal Appl 1988;135:568–80.
[10] Chaudhary MA, Merkin JH, Pop I. Similarity solutions in the free convection boundary-layer flows adjacent to vertical permeable surfaces in porous media. Eur J Mech, B/Fluids 1995;14:217–37.
[11] Elbashbeshy EMA. Heat transfer over a stretching surface with variable surface heat flux. J Phys D: Appl Phys 1998;31:1951–4.
[12] Magyari E, Keller B. Exact solutions for self-similar boundary-layer flows induced by permeable stretching walls. Eur J Mech B—Fluids 2000;19:109–22.
[13] Stewartson K. On the impulsive motion of a flat plate in a viscous fluid (Part I). Quart J Mech 1951;4:182–98.
[14] Stewartson K. On the impulsive motion of a flat plate in a viscous fluid(Part II). Quart J Mech Appl Math 1973;22:143–52.
[15] Hall MG. The boundary layer over an impulsively started flat plate. Proc R Soc A 1969;310:401–14.

[16] Dennis SCR. The motion of a viscous fluid past an impulsively started semi-infinite flat plate. J Inst Math Appl 1972;10:105–17.
[17] Watkins CB. Heat transfer in the boundary layer over an impulsively stearted flat plate. J Heat Transfer 1975;97:282–484.
[18] Seshadri R, Sreeshylan N, Nath G. Unsteady mixed convection flow in the stagnation region of a heated vertical plate due to impulsive motion. Int J Heat Mass Transfer 2002;45:1345–52.
[19] Pop I, Na TY. Mech Res Comm 1996;23:413.
[20] Wang CY, Du G, Miklavcic M, Chang CC. SIAM J Appl Math 1997;57:1.
[21] Nazar N, Amin N, Pop I. Unsteady boundary layer flow due to stretching surface in a rotating fluid. Mech Res Commun 2004;31:121–8.
[22] Williams JC, Rhyne TH. Boundary layer development on a wedge impulsively set into motion. SIAM J Appl Math 1980;38:215–24.
[23] Liao SJ. Beyond perturbation: introduction to the homotopy analysis method. Boca Raton: Chapman & Hall/CRC Press; 2003.
[24] Liao SJ. On the homotopy analysis method for nonlinear problems. Appl Math Comput 2004;147:499–513.
[25] Liao SJ. On the analytic solution of magnetohydrodynamic flows of non-Newtonian fluids over a stretching sheet. J Fluid Mech 2003;488:189–212.
[26] Liao SJ, Campo A. Analytic solutions of the temperature distribution in Blasius viscous flow problems. J Fluid Mech 2002;453:411–25.
[27] Liao SJ. A uniformly valid analytic solution of 2D viscous flow past a semi-infinite flat plate. J Fluid Mech 1999;385:101–28.
[28] Ayub M, Rasheed A, Hayat T. Exact flow of a third grade fluid past a porous plate using homotopy analysis method. Int J Eng Sci 2003;41:2091–103.
[29] Hayat T, Khan M, Ayub M. On the explicit analytic solutions of an Oldroyd 6-constant fluid. Int J Eng Sci 2004;42:123–35.
[30] Hayat T, Khan M, Asghar S. Homotopy analysis of MHD flows of an Oldroyd 8-constant fluid. Acta Mech 2004;168:213–32.
[31] Hayat T, Khan M, Asghar S. Magnetohydrodynamic flow of an Oldroyd 6-constant fluid. Appl Math Comput 2004;155:417–25.
[32] Ifidon EO. Numerical studies of viscous incompressible flow between two rotating concentric spheres. J Appl Math, in press.
[33] Allan FM, Syam MI. On the analytic solutions of the non-homogenous Blasius problem. J Comput Appl Math, in press.